Asian Journal of Chemistry; Vol. 25, No. 1 (2013), 436-440

ASIAN JOURNAL OF CHEMISTRY

http://dx.doi.org/10.14233/ajchem.2013.13147

Spectrophotometric and Voltammetric Studies on the Interaction of 7-Ethyl-10-hydroxycamptothecin (SN-38) as the Metabolized Compound of CPT-11 with ds-DNA

REZA HAJIAN and GUAN H. TAN*

Department of Chemistry, Faculty of Science, University of Malaya, 50603 Kuala Lumpur, Malaysia

*Corresponding author: Tel: +603 7967 4247; E-mail: ghtan@um.edu.my

(*Received*: 30 November 2011; *Accepted*: 28 July 2012) AJC-11895

The interaction of 7-ethyl-10-hydroxycamptothecin (SN-38) and double stranded DNA (ds-DNA) was studied by absorption spectroscopy and cyclic voltammetry at different temperatures. The results revealed that double stranded-DNA caused the hypochromicity of SN-38 absorption spectra at 384 nm. The binding constant K_b and the number of binding sites n, corresponding thermodynamic parameters between SN-38 and double stranded-DNA at different temperatures were calculated. In addition, the van't Hoff plot of 1/T *versus* ln K_b suggests that the SN-38 binds endothermically to double stranded-DNA, which is characterized by large positive enthalpy and entropy changes. The K_b at a low concentration of salt is dominated by electrostatic interaction (99.9 %) while that at a high concentration of salt is weakly controlled by non-electrostatic processes (2.23 %). The intercalation of SN-38 with DNA produces an electrochemically inactive macromolecule complex and the peak current of SN-38 was decreased upon the addition of double stranded-DNA molecules. The diffusion coefficients of SN-38 in the absence and presence of double stranded-DNA was calculated as 4.64×10^{-4} and 4.23×10^{-4} $cm^2 s^{-1}$, respectively.

Key Words: SN-38, Double stranded-DNA, Spectrophotometry, Voltammetry, Thermodynamic parameters.

INTRODUCTION

Camptothecin is a natural, water-insoluble alkaloid produced by two Asian trees, *Camptotheca acuminata*[1] and *Mappia foetida*[2]. In the 1970s, preliminary clinical trials with camptothecin demonstrated promising antitumor activity, for example, in gastric cancer. Unfortunately, there were also severe side effects, including poorly predictable hemorrhagic cystitis, gastrointestinal toxicities and myelosuppression[3-5]. It was not until the early 1980s that the mechanism of antitumor activity of camptothecin was identified as the inhibition of topoisomerase I[6,7]. Researchers then began to modify camptothecin and created a host of analogues with the aim of overcoming the two key factors that hampered clinical application of the parent drug: poor water-solubility and severe toxicity. A number of camptothecin analogues are currently at different stages of clinical development, including topotecan (TPT), irinotecan (CPT-11), lurtotecan (LRT), 9- aminocamptothecin (9-AC), 10-hydroxycamptothecin (SN-38) and 9-nitrocamptothecin (9-NC). Thus far, most clinical experience relates to the water-soluble derivatives topotecan and irinotecan. Irinotecan is converted *in vivo* to its much higher active metabolite, 7-ethyl-10-hydroxy camptothecin (SN-38) by carboxylesterases. Its disposition by the liver and bile is higher than by any other tissue.

Deoxyribonucleic acid plays an important role in the life process because it carries heritage information and instructs the biological synthesis of proteins and enzymes through the process of replication and transcription of genetic information in living cells. Studies on the binding mechanism of some small molecules with DNA have been identified as one of the key topics during the past few decades[8,9]. Moreover, it is of great help to understand the structural properties of DNA, the mutation of genes, the origin of some diseases, the action mechanism of some antitumour and antivirus drugs and, therefore, to design new and more efficient DNA targeted drugs to deal with genetic diseases.

In this respect, our investigation deals with providing a thermodynamic profile, *i.e.* standard free energy (ΔG°), enthalpy (ΔH°) and entropy (ΔS°) changes of the DNA binding of SN-38 using the van't Hoff plot by determining the equilibrium binding constant (K_b) of the DNA binding of SN-38 at various temperatures. Moreover, the effect of salt concentration on the binding constant of SN-38 binding to double stranded-DNA has been studied. The binding affinity of small molecules to DNA theoretically decrease when the salt concentration in the solution increases because ion-pair formation between binding ligand and DNA is less favourable in the solution that contains a high concentration of salt due to competition between cationic binding ligand and cationic metal ion released by the

salt. Therefore, in the present study the salt dependence of the DNA binding of SN-38 to ds-DNA has been characterized by determining its K_b at various concentrations of salt (KCl) using spectrophotometric titration.

As a result of the reaction with ds-DNA, the reduction peaks related to SN-38 shifted to a negative direction and the peak currents decreased. The diffusion coefficients of SN-38 in the absence (D_f) and presence (D_b) of ds-DNA calculated as 4.64×10^{-4} and 4.23×10^{-4} cm^2 s^{-1} respectively. The binding constant ($K = 9.0 \times 10^3$ L mol^{-1}) and binding site size (s = 0.60) of SN-38 interacting with ds-DNA obtained simultaneously by non-linear fit analysis.

EXPERIMENTAL

SN-38 and calf thymus DNA (Sigma, USA) were used without further purification. The SN-38 stock solution of 1×10^{-3} mol L^{-1} was kept away from light to avoid photochemical decomposition and was diluted just before use. The concentration of DNA (1×10^{-3} mol L^{-1}, base pairs) was spectroscopically determined using molar absorption coefficient of 13200 L mol^{-1} cm^{-1} at 260 nm. All reagents were analytical grade and aqueous solutions were prepared using doubly distilled deionized water. Purity of the DNA was checked by monitoring the ratio of the absorbance at 260 nm to that at 280 nm. The solution gave a ratio of >1.8 at A_{260}/A_{280}, which indicates that the DNA was sufficiently protein-free[10].

Phosphate buffer (20 mmol L^{-1}, pH 7.5) and potassium chloride for adjusting the ionic strength were purchased from Fluka (USA). Neutral Red dye stock solution (1.0×10^{-3} mol L^{-1}) was prepared by dissolving its crystals (Sigma-Aldrich) in water and diluted to the required volume.

Cyclic voltammetry studies were carried out by Metrohm instrument, Model 797 VA processor, (Metrohm, Switzerland). The three-electrode system consisted of a HMDE working electrode, an Ag/AgCl-saturated KCl reference electrode and a platinum wire counter electrode. All potentials were referred to the reference electrode.

UV/VIS absorbance spectra were obtained by Shimadzu model 1650 UV-VIS spectrophotometer equipped with a FISONS model HAAKE D1 cell-temperature controller.

RESULTS AND DISCUSSION

Spectrophotometric titration of SN-38 with ds-DNA: The UV-VIS absorption changes of SN-38 in the presence of ds-DNA (with increasing concentration) were examined in the phosphate buffer at pH 7.5 (Fig. 1). SN-38 absorbed with maxima at 264 nm and 382 nm. The intensity of the band at 382 nm decreased gradually as a function of the ds-DNA concentration and a new stronger absorption peak appeared at 280 nm. Moreover, the isosbestic point at about 311 nm indicated that SN-38 could form a stable complex with ds-DNA and the binding was homogeneous.

The degree of hypochromicity (H in %) increases with temperature. For example, the hypochromic effect of SN-38 absorption goes up from 3.41 % to 5.9 % by increasing the temperature from 24 ºC to 33 ºC in the solution containing 2 mM phosphate buffer at pH 7.5 (Table-1).

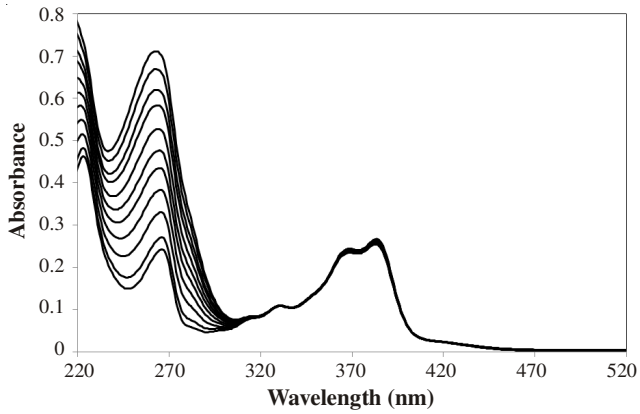

Fig. 1. Absorption spectra of SN-38 in the presence of ds-DNA at different concentrations. C_{DNA} = 0.0, 6.2, 12.4, 18.7, 25.1, 31.6, 38.2, 44.8, 51.6, 53.4, 58.4 and 65.5 μmol L^{-1} for curves 1-15 and C_{CPT-11} = 30.0 μmol L^{-1} in phosphate buffer (0.002 mol L^{-1}, pH 7.5)

TABLE-1
SOME THERMODYNAMIC PARAMETERS FOR THE SN-38 BINDING TO ds-DNA AT VARIOUS TEMPERATURES

T (K)	H* (%)	K_b (L mol^{-1})	ΔH^o (KJ mol^{-1})	ΔS^o (KJ mol^{-1})
297	3.41	1.53×10^3	118.39	463.08
301	5.32	7.39×10^3		
306	5.92	1.12×10^4		
311	4.10	1.56×10^4		

*Hypochromicity

Double-reciprocal method: In order to further investigate the interaction mode of SN-38 with ds-DNA, the binding constant between drug-DNA at different temperatures was calculated according to the double-reciprocal equation[11]:

$$\frac{A_0}{A - A_0} = \frac{\varepsilon_G}{\varepsilon_{H-G} - \varepsilon_G} + \frac{\varepsilon_G}{\varepsilon_{H-G} - \varepsilon_G} \times \frac{1}{K[DNA]} \qquad (1)$$

where, A_0 and A are the absorbances of SN-38 in the absence and presence of DNA, respectively and ε_G and ε_{H-G} are their absorption coefficients. The double reciprocal plots of $A_0/A\text{-}A_0$ *versus* 1/[DNA] were linear and the binding constants were calculated from the ratio of the intercept to the slope equations.

The thermodynamic parameters of DNA-drug complexes are essential for a thorough understanding of the driving forces governing the binding of drugs to DNA. To study the thermodynamic parameter of the ct-DNA binding of SN-38, the binding constant of SN-38 to ds-DNA has been determined at 24, 28, 33 and 38 ºC by spectrophotometric titration and the data were analyzed by Eq. (1). Typical reciprocal plots to determine the binding constant (K_b) at ambient temperature has shown in Fig. 2 and the results of the K_b determination are tabulated in Table-1. The determination of the binding constants at various temperatures provides a good means to indirectly calculate the thermodynamic parameter of the DNA binding through the van't Hoff plot of 1/T *versus* ln K_b in the corresponding temperature range (Fig. 3)[12-14]. As suming that the enthalpy change (ΔH^o) is independent of temperature over the range of employed temperatures, ΔH^o of DNA-binding reaction of SN-38 is immediately obtained from the van't Hoff plot (Table-1). The striking observation of this table is that

SN-38 binds endothermically to ds-DNA because the K_b value increases with temperature.

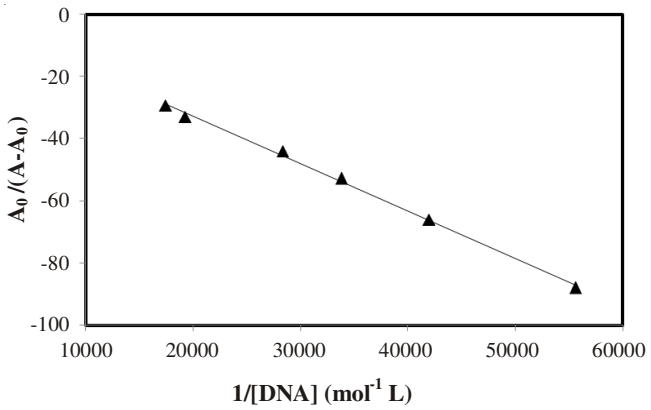

Fig. 2. Typical plots of $A_0/(A-A_0)$ *versus* 1/[ds-DNA] for the determination of the equilibrium binding constant (K_b) based on eqn. (1) of the ds-DNA binding of SN-38 at various temperatures

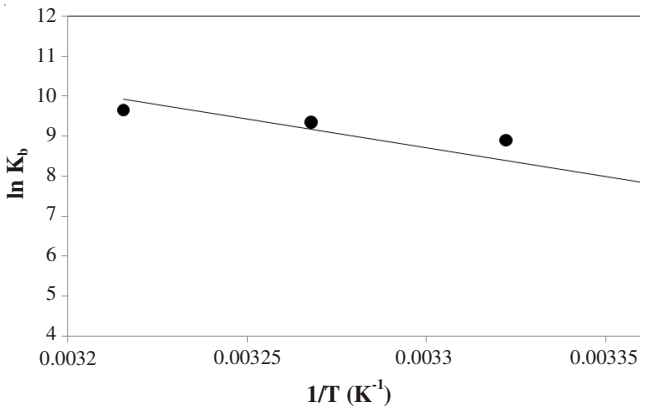

Fig. 3. van't Hoff plot of ln K_b *versus* 1/T for the binding of SN-38 to ds-DNA. All other conditions are similar to Fig. 1

Hill analysis: Several studies on DNA structure[15] show that the influence of a small molecule bound to DNA is unlikely to propagate over a large distance. A large guest, like the present complexes, might contact only one or two base pairs, but sterically exclude the approach of other molecules to nearby sites. Further, an anionic guest like SN-38 would tend to repel another molecule of like charge attempting to bind nearby, but it will alter the local counterion (phospho-diester backbone), which means that the electrostatic free energy of the whole polymer becomes a variable in the analysis of the binding experiment. So the binding at one site along the nucleic acid helix may alter the probability of binding to neighboring sites. To throw light on such possibilities, the present absorption spectral data were replotted according to Hill equation[16],

$$\ln[Y/(1-Y)] = h \ln[X] - \ln D \qquad (2)$$

with $Y = \Delta A/\Delta A\mu$ where $\Delta A\mu$ is the absorbance at the saturation point beyond, which the addition of further DNA causes no appreciable change, [X] is the concentration of DNA (host), K_D is the overall dissociation constant ($1/K_b$) and 'h' is the Hill coefficient, an index of cooperativity. (Non-cooperative systems exhibit h≈1.0, positively cooperative systems h > 1 and negatively cooperative systems h < 1). The interaction of SN-38 with ds-DNA gave satisfactory a straight line with slope (h) of 0.83 (Fig. 4), suggesting the presence of a positive cooperative event in the binding of SN-38, though the nature and mechanism of the cooperative event. Thus the DNA binding of SN-38 at a site of a few base pairs away is enhanced, leading to cooperative effects.

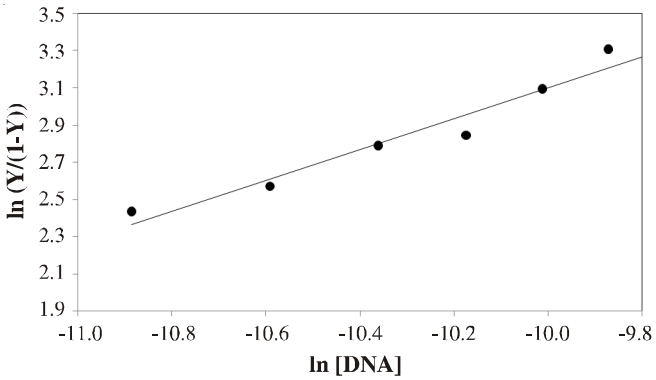

Fig. 4. Hill plot for titration of SN-38 against ln [DNA] (monitored absorbance at 310 nm), giving h = 0.46

Competitive interaction of SN-38 with the NR-DNA complex: Further support for the mode of binding between SN-38 and DNA is given through the competitive interaction of SN-38 and NR with DNA. The observed band of DNA-NR complex at 531 nm gradually decreases in intensity with the increasing concentration of the added SN-38. This band shifted slightly towards the higher wavelengths of the spectrum with the appearance of two new peaks at 388 nm and 418 nm, which increased progressively in intensity (Fig. 5). An isosbestic point at 476 nm provides evidence that a new species is formed during the competitive interaction and that the reaction is homogeneous. The observed changes in intensity and position of the bands with increasing concentration of SN-38 added to the DNA-NR solution, suggested that SN-38 intercalated into the double helix of the DNA by substitution of NR in the DNA-NR system. These changes in the state of intercalation have been observed in several other studies[17,18].

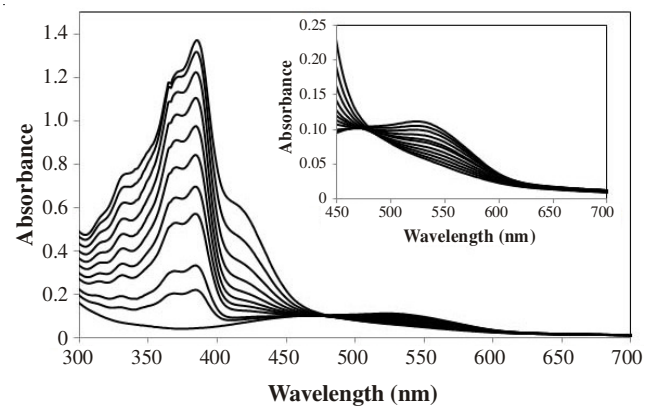

Fig. 5. Absorption spectra of the competitive interaction between SN-38 and NR bonded to ds-DNA in the wavelength ranges of (A) 220-600 nm and (B) 450-700 nm. Conditions: C_{SN-38} = 0.0, 6.7, 13.4, 20.1, 26.8, 33.5, 40.2, 46.9, 53.6, 60.3 and 67.0 μmol L^{-1} for curves 1-11, C_{NR} =10.0 μmol L^{-1} and C_{DNA} = 30.5 μmol L^{-1} in phosphate buffer (0.002 mol L^{-1}, pH 7.5)

Melting studies: The double-helical structure of DNA is remarkably stable due to containing hydrogen bonding and base stacking interactions. Upon increasing the temperature,

the double-helix dissociates to single strands since heat damages those chemical forces. The temperature at which a half of a DNA sample is melted is known as the melting temperature (T_m) and is strongly related to the stability of the double-helical structure[19]. A change of T_m may be observed when an interaction of small molecules with DNA occurs. Intercalative binding can increase the stability of DNA helix and Tm increases by about 5-8 ºC, but the non-intercalation binding causes no obvious increase in T_m[20]. UV-VIS absorption spectroscopy is a general method for determining the melting temperatures. The values of T_m of DNA and SN-38-DNA system were obtained from the transition midpoint of the melting curves based on $A/A_{27\,°C}$ *versus* temperature (T), where, A is the absorbance intensity at 260 nm at different temperatures, $A_{27\,°C}$ is the absorbance intensity at ambient temperature and the temperature ranging is from 40 to 100 ºC. As can be seen from Fig. 6, the T_m of DNA in the absence of SN-38 is 53.0 ºC, but the observed T_m of DNA in the presence of SN-38 is 64 ºC. The interaction of SN-38 with DNA can cause the T_m to be increased, indicated that the stability of DNA was increased in the presence of SN-38.

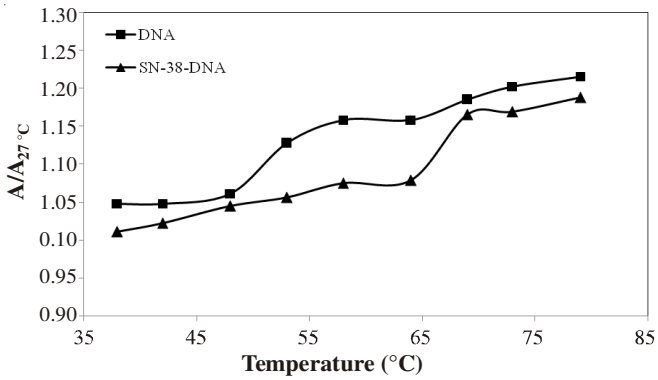

Fig. 6. Thermal denaturation profile of ds-DNA in the absence and presence of SN-38. Conditions: C_{DNA} = 9.2 µmol L^{-1}, C_{SN-38} = 20.0 µmol L^{-1}, phosphate buffer (0.002 mol L_{-1}, pH 7.5)

Electrochemical study

Electrochemical interaction of SN-38 with ds-DNA: Typical cyclic voltammetry behaviour of SN-38 in the absence and presence of DNA has shown in Fig. 7. Addition of DNA to SN-38 solution causes the peak currents of the cyclic voltammetry waves (reduction peaks) to diminish considerably. The binding of SN-38 to ds-DNA should lead to a significant decrease of peak currents due to the formation of SN-38-DNA adduct with a smaller diffusion coefficient compared to the free drug[21,22]. This can be inferred from the significant decrease in the slopes of the linear I_p *vs.* $\nu^{1/2}$ plots in the absence and presence of ds-DNA with the equations of $I_p = 2.97 \times 10^{-7}\nu^{1/2} - 7.59 \times 10^{-9}$ and $I_p = 2.86 \times 10^{-7}\,\nu^{1/2} - 9.52 \times 10^{-9}$ respectively. Additionally the peak potentials ($E_{pc,1}$ and $E_{pc,2}$) shifted to more negative values indicating that the action of SN-38 with DNA may be non electrostatic[23]. The peak potential separations $\Delta E_p = |E_{pc} - E_{pa}|$ are beyond 200 mV indicating an irreversible redox process.

For the irreversible redox reaction of SN-38, the αn_a value (α, the electron transfer coefficient; n_a, the number of electrons involved in the rate-determining step) were calculated as 0.52 and 0.53 for free SN-38 and SN-38-DNA adduct based on the slopes of the Tafel plots. From these values, the diffusion coefficients for SN-38 in the absence ($D^f = 4.62 \times 10^{-4}$ cm^2 s^{-1}) and presence ($D_b = 4.23 \times 10^{-4}$ cm^2 s^{-1}) of ds-DNA were calculated based on eqn. (2), where I_p refers to the peak current (A), n is the electron transfer number, A is the surface area of the electrode (0.0025 cm^2), D_0 is diffusion coefficient (cm^2 s^{-1}), C_o is the concentration (mol cm^{-3}) of SN-38 and ν is scan rate (V s^{-1}).

$$I_p = (2.99\times10^5)n(\alpha n_a)^{1/2} AC_o D_o^{1/2}\nu^{1/2} \quad (2)$$

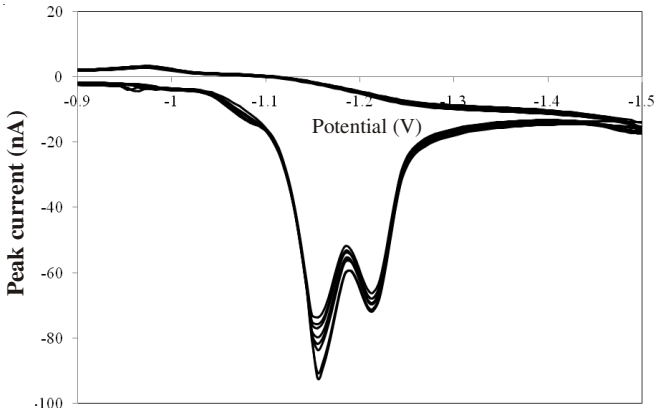

Fig. 7. Cyclic voltammetry of SN-38 in the presence of ds-DNA at different concentrations. C_{DNA} = 0.0, 9.1, 18.0, 26.7, 35.3, 43.7, 51.9 and 60.0 µmol L^{-1} for curves 1-8 and C_{CPT-11} = 10.0 µmol L^{-1} in phosphate buffer (0.002 mol L^{-1}, pH 7.5) and ν = 0.05 V s^{-1}

Binding site and binding site size: For an irreversible reaction at 25 ºC, the peak current (I_p) of SN-38 can be calculated as[24]:

$$I_p = B[(\alpha n_a)_f^{1/2} D_f^{1/2} C_f + (\alpha n_a)_b^{1/2} D_b^{1/2} C_b] \quad (3)$$

where, $B = 2.99 \times 10^5$ $nA\nu^{1/2}$, A is the surface area of the working electrode, C_b and C_f represent the equilibrium concentration of CPT-11 in the presence and absence of DNA and the total concentration of CPT-11 C_t, is:

$$C_t = C_f + C_b \quad (4)$$

Based on the method employed by Carter *et al.*, the binding constant, K, can be expressed as the following form[25,26]:

$$K_b = \frac{C_b}{C_f\left(\frac{[NP]}{2s} - C_b\right)} \quad (5)$$

where, s is the size of binding site in terms of the binding pair (bp) and NP is the DNA concentration. Making appropriate substitutions and eliminating C_b and C_f from eqn. (5), a new equation was obtained:

$$I_p = B\left\{(\alpha n_a)_f^{1/2} D_f^{1/2} C_t + [(\alpha n_a)_b^{1/2} D_b^{1/2} - (\alpha n_a)_f^{1/2} D_f^{1/2}] \times \left[\frac{b - (b^2 - \frac{2K_b^2 C_t [NP]}{s})^{1/2}}{2K_b}\right]\right\} \quad (6)$$

where, $b = 1 + K_b c_t + K_b[NP]/2s$. Since I_p, C_t and [NP] are experimentally measurable and $(an_a)_f$, $(an_a)_b$, D_f and D_b have already been acquired as mentioned above, the binding constant (K_b) and binding site size (s) of the CPT-11-DNA can be obtained from a nonlinear regression analysis of the experimental data (I_p-[DNA] plot) according to eqn. (6). For

the binding curve (Fig. 8), a nonlinear fit analysis yielded $K_b = 9.0 \times 10^3$ L mol^{-1} and s = 0.6 bp.

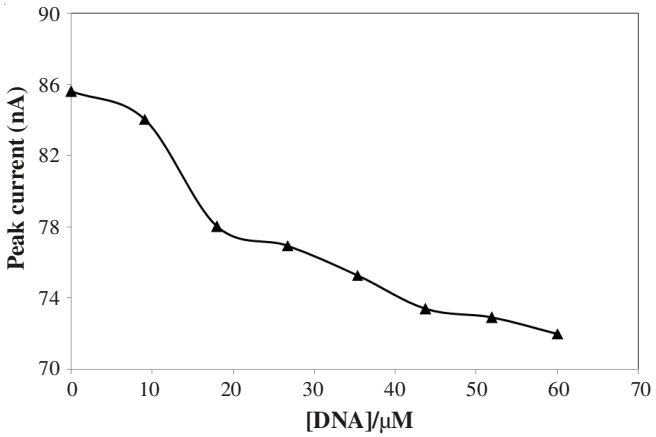

Fig. 8. Binding curve of SN-38 in the presence of ds-DNA at different concentrations. C_{DNA}=0.0, 9.1, 18.0, 26.7, 35.3, 43.7, 51.9 and 60.0 μmol L^{-1} and C_{SN-38} =10.0 μmol L^{-1} in phosphate buffer (0.002 mol L^{-1}, pH 7.5) and ν = 0.05 V s^{-1}

Conclusion

The binding interactions between SN-38 as the metabolite compound of CPT-11 and calf thymus DNA have been investigated using UV-VIS absorption and cyclic voltammetry. The results indicated that SN-38 can bind to DNA and the major binding mode is intercalative binding. These results were further supported by DNA melting studies and viscosity measurements. The binding constants of SN-38 to DNA were obtained at three different temperatures. The calculated thermodynamic parameters suggested that the binding of SN-38 to DNA was driven mainly by hydrogen bonds and van der Waals forces. A competitive reaction of SN-38 and NR with DNA monitored by UV-VIS spectroscopy showed that the intercalated NR was displaced from the DNA-NR system by SN-38.

In addition, the diffusion coefficients of free and bounded SN-38 to DNA (D_f and D_b), binding constant (K_b) and binding site size (s) were calculated using the slope of the I_p *vs.* $\nu^{0.5}$ plots and non-linear fit analysis, which is suitable to study the interaction of DNA with irreversible electroactive molecules.

ACKNOWLEDGEMENTS

The authors gratefully acknowledge the support of this work by Gachsaran branch, Islamic Azad University.

REFERENCES

1. M.E. Wall, M.C. Wani, C.E. Cook, K.H. Palmer, A.T. McPhail and G.A. Sim, *J. Am. Chem. Soc*., **88**, 3888 (1966).
2. T.R. Govindachari and N. Visnawathan, *Phytochemistry*, **11**, 3529 (1972).
3. J.A. Gottlieb, A.M. Guarino, J.B. Call, V.T. Oliverio and J.B. Block, *Cancer Chemother. Rep*., **54**, 461 (1970).
4. C.G. Moertel, A.J. Schutt, R.J. Reiterneier and R.G. Hahn, *Cancer Chemother. Rep*., **56**, 95 (1972).
5. F.M. Muggia, P.J. Creaven, H.H. Hansen, M.H. Cohen and O.S. Selawry, *Cancer Chemother. Rep*., **56**, 515 (1972).
6. Y.H. Hsiang, R. Hertzberg, S. Hecht and L.F. Liu, *J. Biol. Chem*., **260**, 14873 (1985).
7. Y.-H. Hsiang and L.F. Liu, *Cancer Res*., **48**, 1722 (1988).
8. Q.Y. Chen, D.H. Hi, Y. Zhao and J.X. Guo, *Analyst*, **124**, 901 (1999).
9. R. Hajian, N. Iravani, F. Ghanbari and N. Shams, *Asian J. Chem.*, **24**, 3656 (2012).
10. S. Mahadevan and M. Palaniandavar, *Inorg. Chem*., **37**, 693 (1998).
11. M. Purcell, J.F. Neault and T. Riahi, *Biochim. Biophys. Acta*, **1478**, 61 (2000).
12. N.Y. Mudasir and H. Inoue, *J. Inorg. Biochem*., **77**, 239 (1999).
13. D.H. Tjahjono, T. Akutsu, N. Yoshioka and H. Inoue, *Biochim. Biophys. Acta*, **1472**, 333 (1999).
14. D.H. Tjahjono, T. Yamamoto, S. Ichimoto, N. Yoshioka and H. Inoue, *J. Chem. Soc. Perkin Trans. I*, 3077 (2000).
15. J.R. Quintana, K. Grzeskowiak, K. Yanagi and R.E. Dickerson, *J. Mol. Biol*., **379**, 225 (1992).
16. R.C. Petter, J.S. Salek, C.T. Sikorski, G. Kumaravel and F.T. Lin, *J. Am. Chem. Soc*., **112**, 3860 (1990).
17. Y.N. Ni, D.Q. Lin and S. Kokot, *Talanta*, **65**, 1295 (2005).
18. C.V. Kumar, R.S. Turner and E.H. Asuncion, *J. Photochem. Photobiol. A-Chem*., **74**, 231 (1993).
19. U. Chaveerach, A. Meenongwa, Y. Trongpanich, C. Soikum and P. Chaveerach, *Polyhedron*, **29**, 731 (2010).
20. S.Y. Bi, H.Q. Zhang, C.Y. Qiao, Y. Sun and C.M. Liu, *Spectrochim. Acta,* **A 69**, 123 (2008).
21. I.S. Shehatta and M.S. Ibrahim, *Can. J. Chem*., **79**, 1431 (2001).
22. M. Aslanoglu and G. Ayne, *Anal. Bioanal. Chem.*, **380**, 658 (2004).
23. D.W. Pang and H.D. Abruna, *Anal. Chem*., **70**, 3162 (1998).
24. S.F. Wang, T.Z. Peng and C.F. Yang, *Biophys. Chem*., **104**, 239 (2003).
25. M.T. Carter, M. Rodriguez and A.J. Bard, *J. Am. Chem. Soc*., **111**, 8901 (1989).
26. D.T. Breslin, J.E. Coury, J.R. Anderson, L. McFail-Isom, Y.Z. Kan, L.D. Williams, L.A. Bottomle and G.B. Schuster, *J. Am. Chem. Soc*., **119**, 5043 (1997).